

Supplementary document for

Strain sensing efficiency of hierarchical nano-engineered smart twill-weave composites: Evaluations using multiscale numerical simulations

Sumeru Nayak¹, Sumanta Das^{2}*

¹Graduate Student, Civil and Environmental Engineering, University of Rhode Island, Kingston, RI 02881, United States

^{2}Assistant Professor, Civil and Environmental Engineering, University of Rhode Island, Kingston, RI 02881, United States, Email: sumanta_das@uri.edu (corresponding author)*

<https://doi.org/10.1016/j.compstruct.2020.112905>

A. Mesh Generation

The procedure of meshing involves definition of free mesh for the matrix cube with the embedded inclusions (here, fibers). The periodic unit cell geometry comprises a cubic boundary with embedded inclusions. The meshing procedure culminates in a conformal tetrahedral mesh (with mappable nodes on opposite faces) in the periodic unit cell thus facilitating PBC application. A brief outline of the technique is mentioned herewith. The sequential process initiates with generation of a periodic surface mesh on each face of the cube. Thereafter, a surface mesh is generated on each inclusion followed by construction of a tetrahedral volume mesh inside the inclusion. Having generated the periodic surface mesh on the cube and the inclusion surface, a volume mesh is generated around every inclusion and the cube by inverting the orientation of the inclusion surface mesh triangles. The volume meshes thus generated (one inside the fiber and the other between the inclusion and the cube) are united to form a conformal mesh. For the generation of cohesive elements at the interface of the inclusions and the matrix, the coordinates of the nodes on the surface of the inclusions are duplicated followed by a renumbering of nodes which are further connected to form elements with zero thickness. Needless to mention, the shape of the cohesive element is triangular (with a constant thickness initially zero) for ensuring compatibility with the tetrahedral mesh of the fibers and matrix surrounding it. The procedure for generation of surface meshes and subsequent volume meshes followed by the union is illustrated in a flowchart (See Figure A.1) and described hereafter.

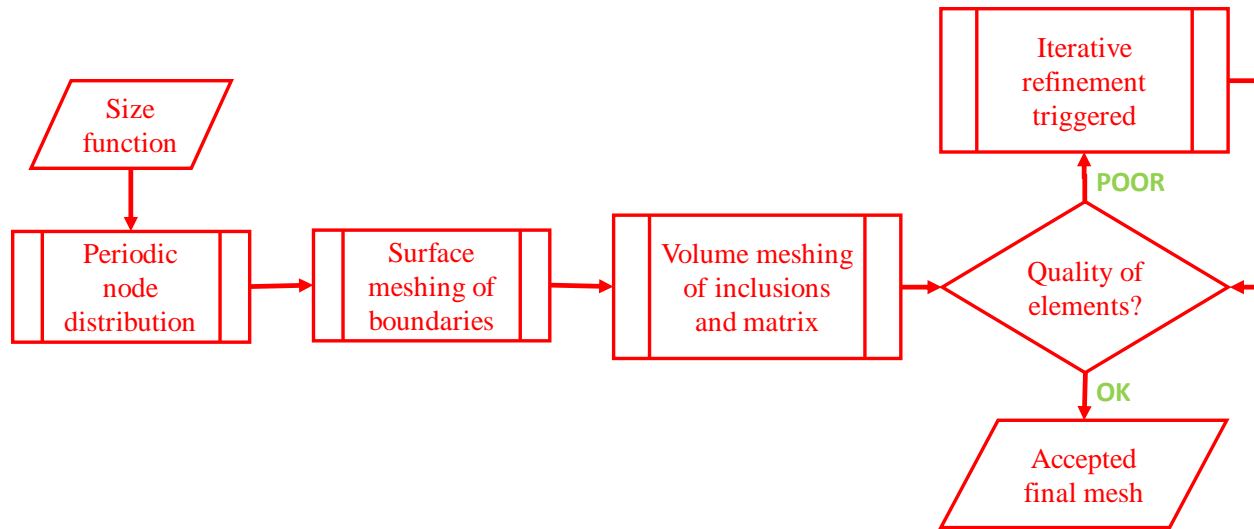


Figure A.1. Meshing procedure adopted for inclusion-matrix periodic unit cells

The first step involving generation of surface meshes on each face of the periodic unit cell initiate with periodic distribution of nodes on the edges of each of the base-faces of the cube (one face per XY, XZ and YZ planes) which are appropriately translated to construct the opposite faces (along XY, YZ and XZ planes) of the cube. The second step of generating surface mesh on the inclusion surface is constructed by defining nodes on the lateral surface and the faces of the inclusions (for cylindrical fibers as adopted in the current study). The third step generates a volume tetrahedral mesh inside each inclusion with respect to the surface mesh. The fourth step involves renumbering of the nodes on the surface of the inclusion so as to invert the orientation of the triangles of the surface mesh on the inclusion with respect to the volume mesh inside the inclusion. With the reoriented inclusion surface mesh, a volume mesh is generated in the region between each inclusion and the cube. The final step ensures compatibility of the two sets of volume meshes (one set inside the inclusion and the other set in the region between the inclusion and the cube) at their shared boundary which is achieved by consecutive renumbering of nodes on the surface of the inclusion (which are shared by both sets of volume meshes) followed by the renumbering of nodes inside each inclusion; thus producing a conformal volume mesh with appropriate connectivity of nodes. The meshing procedure is summarized in a flowchart (See Figure A.1). Having obtained the conformal mesh, the PBC are applied on the unit cell. Towards that end, three sets of nodes are extracted. This is required to prevent over constraining of shared nodes (note that edge nodes are shared by adjacent faces while vertices are shared by orthogonal edges). The sets of nodes are as follows. First set: vertex nodes (8 in number for cubic cells), second set: edge nodes for each of the 8 edges on the cell and third set: nodes on each of the 6 faces. The second and third sets are further categorized as per their orientations (parallel to x, y and z directions). In a manner similar to the first step of mesh generation, the base-faces (along XY, XZ and YZ planes) are

constrained to the opposite faces for a trivial application of PBC. The constraint equations can be found in [1,2]. It is to be noted that definition of reference points (distinct from the geometry) facilitates the application of the PBC whereby the displacements can be applied on the reference points. A similar methodology of conformal mesh generation is adopted for the 2x2 textile weave unit cell that generates tetrahedral solid elements in the yarns and the surrounding matrix with a similar PBC implementation.

B. Mesh Convergence

The mesh convergence studies for each scale: CNT-PSS scale, GF-epoxy unit cell and 2x2 tow-matrix unit cell are shown in Figures B.1(a), (b) and (c) respectively.

For the CNT-PSS unit cell, Figure B.1(a) shows the effect of element size on the homogenized stress-strain behavior. The sizes of the elements are chosen with respect to the mean fiber diameter. In order to capture the geometry of the fiber, the size of the elements are chosen below $0.8R^f$ (where R^f is the radius of the fiber). From Figure B.1(a), it can be observed that choosing an element size below $0.2R^f$ causes insignificant change in results. The corresponding number of elements are 1642270.

For the glass fiber-PSS matrix unit cell, Figure B.1(b) shows the variation of computed effective properties with the number of elements. An element size is chosen to adequately represent the geometry (upper limit being $0.8R^f$). From Figure B.1(b), it can be observed that the optimum number of elements lies beyond 3×10^5 . Thus, the chosen element size is $0.25R^f$ that generates 331836 elements.

For the 2x2 weave unit cell, Figure B.1(c) shows the homogenized stress-strain behavior for the 2x2 weave unit cell with different number of elements (N_{elem}). The chosen element size for the mesh is governed by the thickness of the unit cell (note that each yarn is 0.12mm thick). The matrix pockets between adjacent tows and the regions of crossovers govern the minimum element size. The mesh convergence study (see Figure B.1(c)) shows the optimum element size as 0.022 mm that generates 2223642 elements. Further refinement increases computational burden without significantly affecting results.

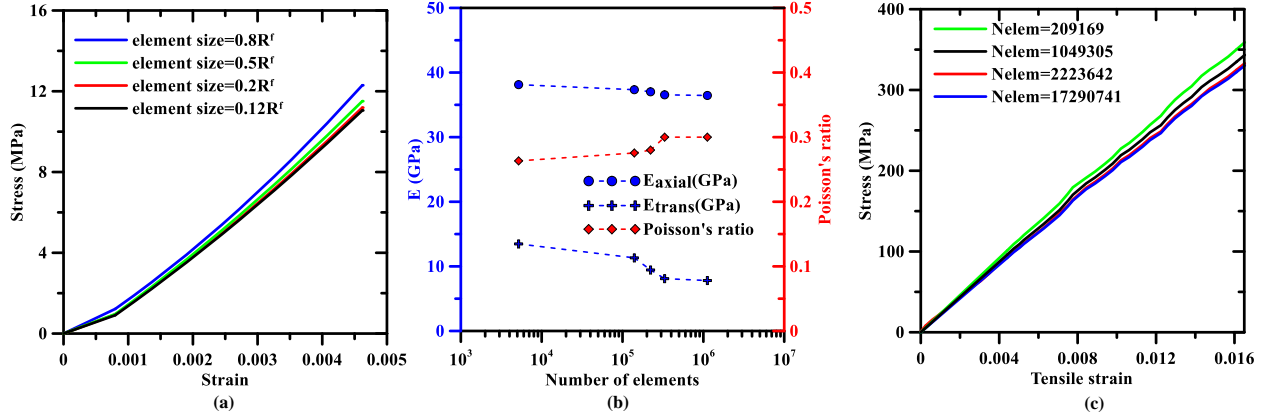


Figure B.1. Mesh convergence studies for (a) CNT-PSS unit cell [stress-strain response for different element sizes wrt R_f : mean radius of fiber] (b) Glass fiber-PSS unit cell [computed effective properties vs number of elements] and (c) 2x2 weave unit cell [stress-strain response for Nelem: number of elements]

C. RVE size sensitivity study for CNT-PSS nanocomposite

In order to generate a representative unit cell for the CNTs randomly dispersed in PSS, an RVE size sensitivity study for the same is carried out. This ensures that the RVE sizes are large enough for adequate representation of features. It is to be noted that the volume fraction of the fibers being fixed at 0.038, a larger RVE size accommodates a higher number of inclusions to achieve that fixed volume fraction. Additionally, the volume fraction of CNTs in the study is adopted as per the experimental procedure and is higher than the percolating volume threshold of 0.028. Towards establishing the adequate RVE size, ten RVEs are generated for every RVE size. Thereafter, uniaxial tension simulations are carried out along each of the orthogonal directions to calculate the homogenized Young's modulus for every combination. Figure C.1 shows the variation of the predicted properties with RVE size (edge length of cubic RVE). It can be observed that the fluctuations represented by error bars are high for RVEs of smaller sizes which eventually die out with a sufficiently large RVE size. Additionally, the directional properties converge for RVE sizes ≥ 300 nm. Thus, the chosen RVE size is 300nm for adequately capturing the isotropic behavior of the CNT-PSS nanocomposite. The chosen size invokes a trade-off between computational expense and prediction efficiency.

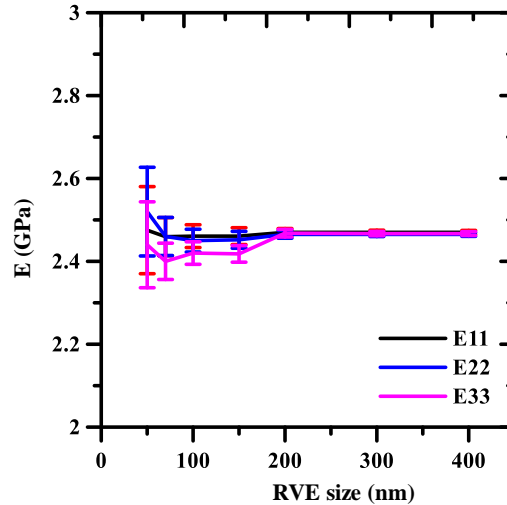


Figure C.1 Influence of RVE size on the predicted E11, E22 and E33 along orthogonal directions for CNT-PSS nanocomposite

D. Software and Tools

The FE solver ABAQUS™ is used to carry out the computations. Custom pre-processors are coded in Python to generate RVEs for CNT-PSS and GF-PSS unit cells. Python API with FreeCAD is used to generate the geometries in Parasolid format which can be imported to ABAQUS CAE. A python 2.7 script in ABAQUS imports the geometry, inserts boundary triangles, generates volume meshes for every part and implements cohesive interactions. Constraints enforcing PBC and ties are generated as well. The generated odb are analyzed by a post-processor coded in Python. For the 2x2 textile, TexGen© GUI (powered by Python 2.7) is used to generate a 2x2 weave unit cell which is exported as a volume mesh with periodic conditions. The element positions and orientations (also exported from TexGen) are used to define local material orientations (note that warp and weft yarns are orthogonal to each other while the fiber bundle has distinct axial, transverse and out-of-plane material properties). Constraints and suitable BCs are thereafter implemented. The simulations are run from ABAQUS Command and the generated odb are analyzed. The material models for ABAQUS are coded in FORTRAN as user defined subroutines. The interpolation maps for translating mechanical responses to strain-induced electrical property inputs are generated in MATLAB. This facilitates an multi-physics based implementation of piezoresistive behavior.

REFERENCES

- [1] Wang R, Zhang L, Hu D, Liu C, Shen X, Cho C, et al. A novel approach to impose periodic boundary condition on braided composite RVE model based on RPIM. *Composite Structures* 2017;163:77–88. <https://doi.org/10.1016/j.compstruct.2016.12.032>.
- [2] Tian W, Qi L, Chao X, Liang J, Fu MW. Numerical evaluation on the effective thermal conductivity of the composites with discontinuous inclusions: Periodic boundary condition and its numerical

algorithm. *International Journal of Heat and Mass Transfer* 2019;134:735–51.
<https://doi.org/10.1016/j.ijheatmasstransfer.2019.01.072>.